Journal of Sustainability Science and Management
Volume 8 *Number* 2, December 2013: 150-160
ISSN: 1823-8556

OIL-PALM SHELL ACTIVATED CARBON PRODUCTION USING CO_2 EMISSION FROM $CaCO_3$ CALCINATION

MAHMOOD SULAIMAN*, MARZUKI ISMAIL AND AHMAD JUSOH

Department of Engineering Science, Faculty of Science and Technology, Universiti Malaysia Terengganu, Mengabang Telipot, 21030 Kuala Terengganu, Malaysia.

**Corresponding author: mahmood@umt.edu.my*

Abstract: The need to capture CO_2 emission, the major factor in global warming, from stationary plant is crucial for Malaysia. Cement manufacturing contribute a significant amount of this emission due to its calcination process of the limestone. In this study, this CO_2 emission was used to activate the oil-palm shell (OPS), which is an abundance waste from palm oil refinery plant. The efficiency of the C-CO_2 reaction of the synergetic process was calculated to determine the amount of CO_2 emission being used in activating the OPS. The carbonized OPS was heated with $CaCO_3$ in the furnace. The remaining $CaCO_3$ and the generated oil palm shell activated carbon (OPSAC) weight were measured. The column test was used to determine the adsorption capability of the generated OPSAC. It was found that the CO_2 is released slowly at higher than permissible calcination temperature of 848 ^oC and increased rapidly as the temperature increased. High C-CO_2 reaction efficiencies above 70 % are attained at 850 ^oC or with equal weight ratio between $CaCO_3$ and carbonized OPS. The highest experimental adsorption capability at 31.38 mg/g was achieved using 45g $CaCO_3$ at 950 ^oC, compared to 18 mg/g using commercial activated Oil Palm Shell activated carbon (OPSAC). The Scanning Electron Microscopy (SEM) verified the increment of the pore area thus the surface area of the generated activated carbon. The experiment proved that the CO_2 emission from the calcination can be eliminated by activating the oil palm shell waste.

KEYWORDS: Oil-palm shell, activated carbon, activation, calcination, adsorption.

Introduction

In Malaysia, Carbon Dioxide (CO_2) emissions represented about 75% of the total greenhouse gas emissions in 2000, compared to 69% in the Initial National Communication (Second National Communication, 2011). This CO_2 emission has increased 118% to 120,475 thousand metric tons from 1990 to 1998, against only 8% in global change. There are two major sources for CO_2 emissions in Malaysia, the transportation sector and power industries, each at 28% and cement manufacturing contributed 4% of the emission (World Research Institute, 1998). In the cement manufacturing, CO_2 emission releases are due to its calcination process of Calcium Carbonate ($CaCO_3$) (Stanmore *et al.,* 2005). The Prime Minister of Malaysia mentioned in the 15th Conference of the Parties that Malaysia is adopting an indicator of a voluntary reduction of up to 40% in terms of carbon emissions intensity of GDP by the year 2020. Meanwhile, the extension of the palm oil industry was followed by the production of massive quantities of by-products at plantation grounds, oil mills and plant. It is estimated 4 million tonnes of the shell is wasted in 2007 or 6-7% of total Fresh Fruit Bunch output (Malaysia Palm Oil Board, 2007; Harimi *et al*., 2004). As palm oil shell is easily obtained and the cost is low, rather than just dumping as a waste, it is somehow reasonable to make use of them as a filter or adsorbent. It is an added advantage to the oil palm industry if the excess shell can be turned into applicable and valuable products. Activated carbon is widely used due to their ability to adsorb a large diversity of compounds from both gaseous and liquid streams (Lua *et al.,* 2001).

There are growing interests in research for renewable and cheaper activated carbon which can virtually manufactured from any carbonaceous precursor. Gas activation such as CO_2 creates more micropores and renders it more suitable for gas adsorption application. CO_2 gas activation is proposed to substitute Zinc Chloride ($ZnCl_2$) activation due to environmental waste issue. Previous study of the oil palm shell activation by CO_2 gas is using a supply from a pressurized tank (Guo *et al*., 2001). Meanwhile, the use of CO_2 gas from supplied tanks also generates another issue as the excess gas molecules that are not take part in the activation will be released in the atmosphere. The purpose of this study is to investigate the synergetic process of the CO_2 removal from $CaCO_3$ calcination by the activation of oil-palm shell using the same CO_2 gas. The effects of activation temperature, oil-palm shell weight ratio to $CaCO_3$ and activation retention time will be investigated. The results of the produced CO_2, carbon weight loss and oxidation efficiency will be measured. The adsorption performance of the produced activated carbon will be compared to the commercial OPSAC.

Material and Methods

The raw oil palm shell is obtained from local refinery plant. The commercial activated carbon sample is bought from Soon Ngai Engineering Sdn. Bhd. The raw OPS is cleaned with de-ionized water and heated in the furnace using a closed crucible at 700 °C for 2 hours. The content of the volatile matters was reduced from 77% to 36% (Guo *et al*., 2001). A 15 gram sample of carbonized OPS was weighed in a 50ml crucible using an analytical balance. Then, the weighed crucible was put into a series of 250ml crucible that contain with 0 gram, 15 gram, 30 gram and 45 gram of $CaCO_3$. The 250 ml crucible was then closed with crucible lid, leaving the 50 ml crucible inside it opened, as shown in Figure 1. The whole crucible was put into the furnace and heated at 850 °C, 900 °C, 950 °C and 1000 °C up to 10 hours with hourly interval. The weight of the generated activated samples and the remaining calcinated calcium carbonate/ calcium oxide were recorded. A column model is used to study the adsorption capability of the generated OPSAC in adsorbing CO_2 gas adsorbate as shown in Figure 2. CO_2 gas was injected into adsorption column B. The flowrate was controlled using flowmeter C. The remaining of the adsorbed CO_2 gas was detected by CO_2 sensor A, the Kanomax IAQ. A 1000 ppm CO_2 gas as adsorbate is purchased from Draeger Safety. The experiments were carried at 1 atm. and 25°C. Meanwhile, the surface of the samples is scanned using JSM 6360 LA scanning electron microscope (SEM) at Institute of Oceanography (INOS), Universiti Malaysia Terengganu.

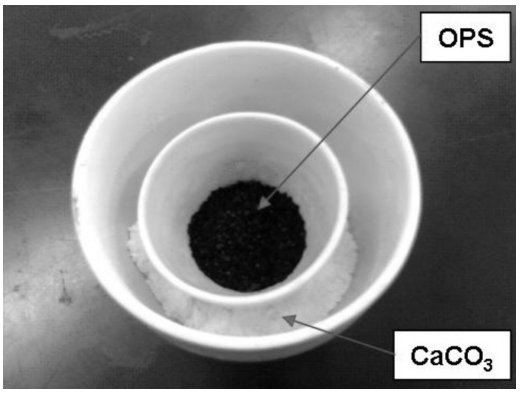

Figure 1: Arrangement of the Carbonized OPS and $CaCO_3$ in the Crucible.

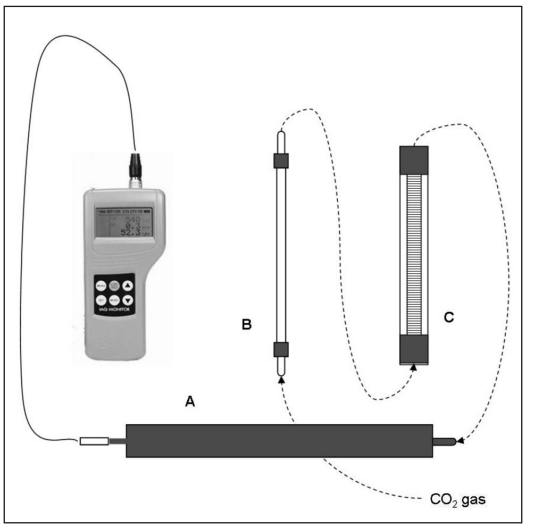

Figure 2: Model for Adsorption Experiment.

Results and Discussion

Surface Scan of the Generated OPSAC

In this surface scan study, the OPS were activated at 900 °C with 30 gram of $CaCO_3$ for 2hr, 4hr and 10hr respectively. As a comparison, Figure 3(a) is the image of the commercially available OPSAC. Figure 3(b) shows the OPS when activated for 2 hours. The pores quantity at the surface becomes more apparent than commercial OPSAC with creation of smaller pores on the surface. The average pore diameter is 0.827±0.18 µm, compared to 0.733±0.21 µm for commercial OPSAC. As the activation time increased to 4 hours as in Figure 3(c), the diameter of the pores is also increased to the point where the smaller pores are visible inside the larger pores. This proves that as the entrance diameter of the pore increased, so does the existence of additional smaller pores inside it. The pores diameter also becomes larger and starting to merge between them. The average pore diameter increased to 1.275±0.26 µm. At certain area, the mesopores and micropores started to appear on the surface. As a result, the total surface area of the pores is also increased (Guo *et al.,* 2002). As the activation time continues, the release of the volatile matters and carbon from C-CO_2 reaction is so severe that the surface was totally covered with mesopores and micropores, as shown in Figure 3(d). The average pore diameter is 1.63±0.4 µm.

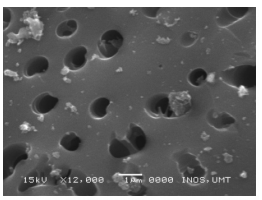

Figure 3(a)

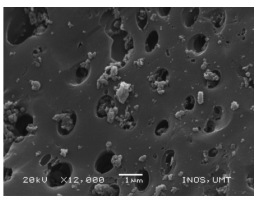

Figure 3(b)

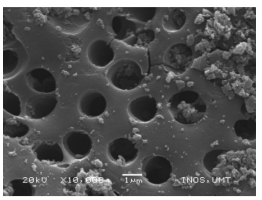

Figure 3(c)

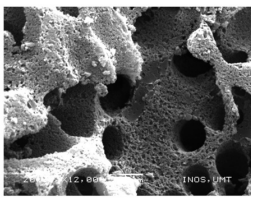

Figure 3(d)

SEM scanned surface of the OPSAC at 10000x/ 12000x.

Carbon Dioxide Production

The CO_2 production due to calcination is measured. The amount of the CO_2 in mol is calculated using chemical equation as below.

$CaCO_3 \rightarrow CaO + CO_2$

From the calcination process, the remaining solid or powder contain both untreated $CaCO_3$ and produced CaO.

Thus,
Untreated $CaCO_3$ + produced CaO = total remaining
[Pretreated $CaCO_3$ – treated $CaCO_3$] + produced CaO = total remaining
Pretreated $CaCO_3$ - [x.mol CO_2 x 44 $g.mol^{-1}$] = total remaining
Thus, x.mol CO_2 = (pretreated $CaCO_3$ – total remaining)/44

The result of released CO_2 (in mol) from the calcination process against time for 45 gram of $CaCO_3$ is shown in Figure 4. At 850 °C, the CO_2 releases continue even after 10 hours. This is due to the temperature is too close to permissible calcination temperature at 848 °C. As the calcination temperature increase to 900 °C, 950 °C and 1000 °C, the time to reach saturation points are reduced significantly. The CO_2 release is higher as it reached significantly closer to the predicted values. The reciprocal-x model is best suited for the relationship of the data. The saturation points were determined and its respective turning point times at 95% of maximum values.

The CO_2 releases for 15 and 30 gram have shown similar trend as shown in table 1. The correlation coefficient is higher than 0.85, indicating a strong relationship between the CO_2 produced and the heating time, except for 15 g $CaCO_3$ at 950 °C and 1000 °C, where the relationship is best suited to linear. This is due to immediate release of CO_2 within the first hour at a very high heating temperature. As the calcination temperature continues to increase, the time to reach for CO_2 to be released almost completely is reduced drastically. Beyond saturation time, no more CO_2 is released. Thus, the activation of the OPS, if continues, is predominantly by heat. Higher CO_2 production is also contributed by a higher amount of $CaCO_3$.

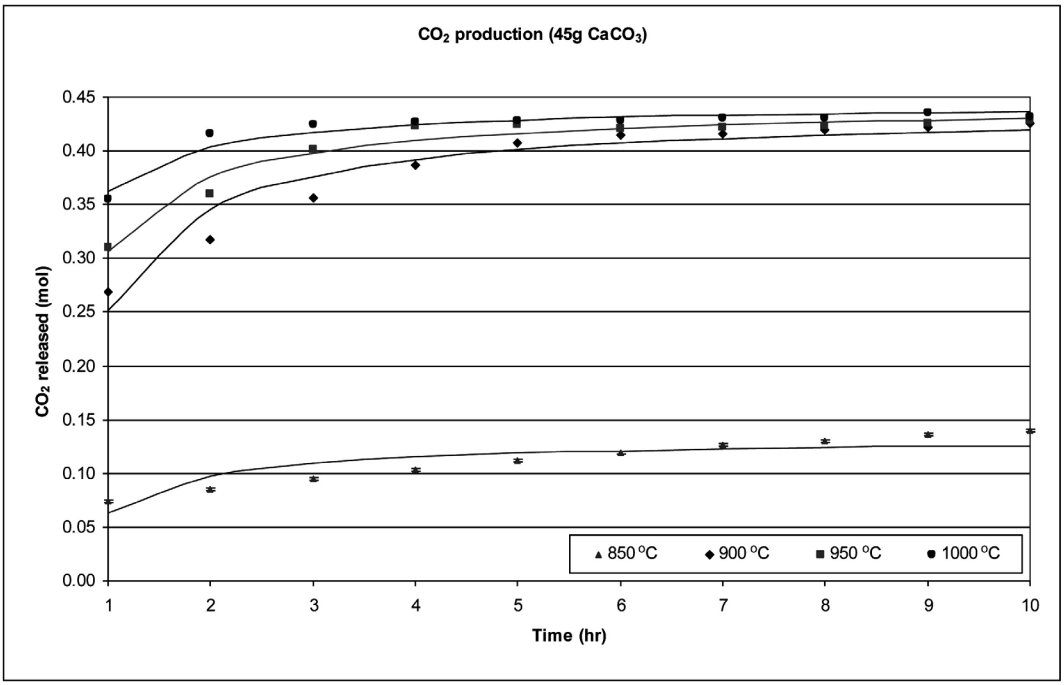

Figure 4: CO_2 Production (mol), 45 gram $CaCO_3$.

Table 1: CO_2 Production Statistical Result.

		15 g $CaCO_3$	30 g $CaCO_3$	45 g $CaCO_3$
850 °C	CO_2 produced at 95% saturation(mol)	0.08	0.11	0.13
	Time (hour)	7.9	10.16	10.53
	Correlation Coefficient	0.88	0.88	0.87
	CO_2 releases efficiency (%)	55.48%	36.09%	27.99%
900 °C	CO_2 produced at 95% saturation(mol)	0.124	0.272	0.416
	Time (hour)	3.97	6.93	8.48
	Correlation Coefficient	0.98	0.96	0.97
	CO_2 releases efficiency (%)	82.81%	90.59%	92.46%
950 °C	CO_2 produced at 95% saturation(mol)	0.126	0.274	0.422
	Time (hour)	0.6	4.08	6.18
	Correlation Coefficient	0.56	0.99	0.98
	CO_2 releases efficiency (%)	84.03%	91.20%	93.72%
1000 °C	CO_2 produced at 95% saturation(mol)	0.134	0.284	0.423
	Time (hour)	0.75	2.33	3.7
	Correlation Coefficient	0.56	0.92	0.97
	CO_2 releases efficiency (%)	89.44%	94.68%	93.93%

Activation-calcination Results

During the activation of the OPS, the heat activation was supplemented by CO_2 gas activation from the $CaCO_3$ calcination. The heat contributed to loss of volatile matter while the CO_2 oxidised the carbon of the OPS (Lua *et al.,* 2001). Thus, the amount of the carbon loss due to CO_2 oxidation can be compared to the OPSAC weight generated by heat alone. While C-CO_2 reaction efficiencies is the amount of carbon loss against the CO_2 generated by the calcination. The elemental studies of the generated OPSAC were not studied in this experiment since the main interest is to study the impact of the calcination on the activation and ultimately the capture of the CO_2 emission and the adsorption result of the OPSAC. Besides, the activation studies of the OPS was well performed in other literatures.

The amount of OPS weight loss due to activation and the C-CO_2 oxidation efficiency was calculated. Figure 5 shows the effects on OPS weight loss activated at 850 ^oC. The weight loss increased almost at steady increment as the activation time increased. The activation using $CaCO_3$ contributes further weight loss compared to activation using the heat alone. Due to limited CO_2 gas output, the OPS loss increment up to 10 hours is dominantly from the heat, thus the curve is close to linear with R^2 is 98.65%, 98.17%, 97.73% and 97.65% for 0 g, 15 g, 30 g and 45 g $CaCO_3$ weight respectively. Due to heat, the loss is also dominantly the release of volatile matters. Plus, the CO_2 output between the carbonate weight samples are very close. So, the weight loss among the samples is very close especially between 30 g and 45 g samples. The activation with $CaCO_3$ still continues at 10 hour since the release of the CO_2 still occurs. Thus, at 850 ^oC, the activation is both by heat and CO_2 gas along within activation time. While, Figure 6 shows the result of the OPS weight loss using 45 gram of $CaCO_3$. As the activation temperature increase, so does the weight loss. However, the weight loss started to saturate at 950 ^oC and 1000 ^oC especially towards the end of activation time.

The main interest is to see the advantage of the CO_2 activation compared to heat only activation. The OPS weight loss due to activation by $CaCO_3$ weight is subtracted to each result of heat activation alone. A series of curves of the loss due to CO_2 against activation time showed the saturation point and its respective times.

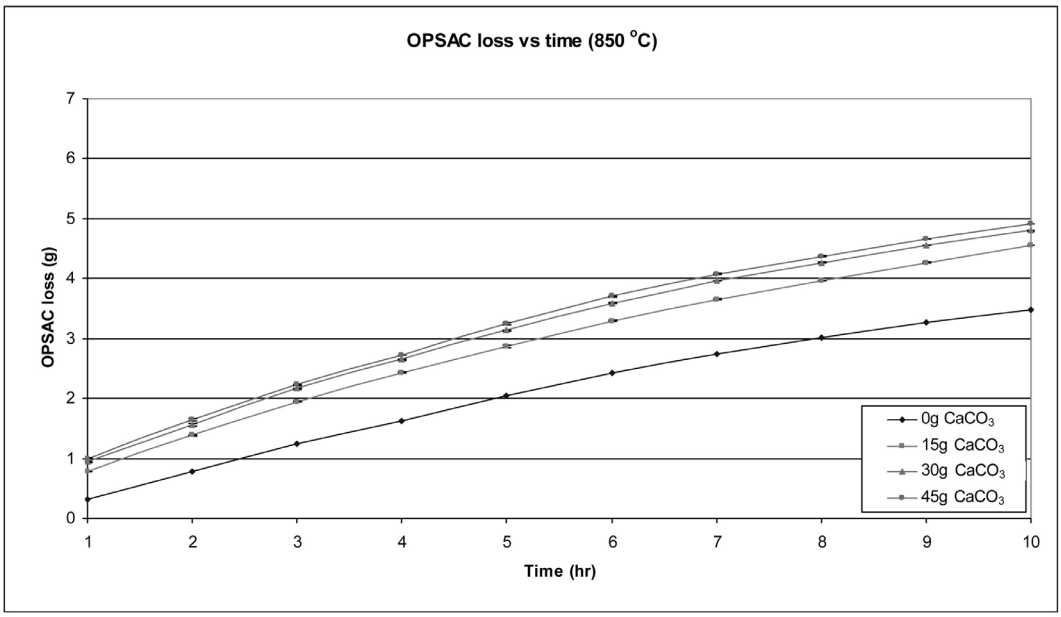

Figure 5: OPS Weight Loss heated at 850 ^oC.

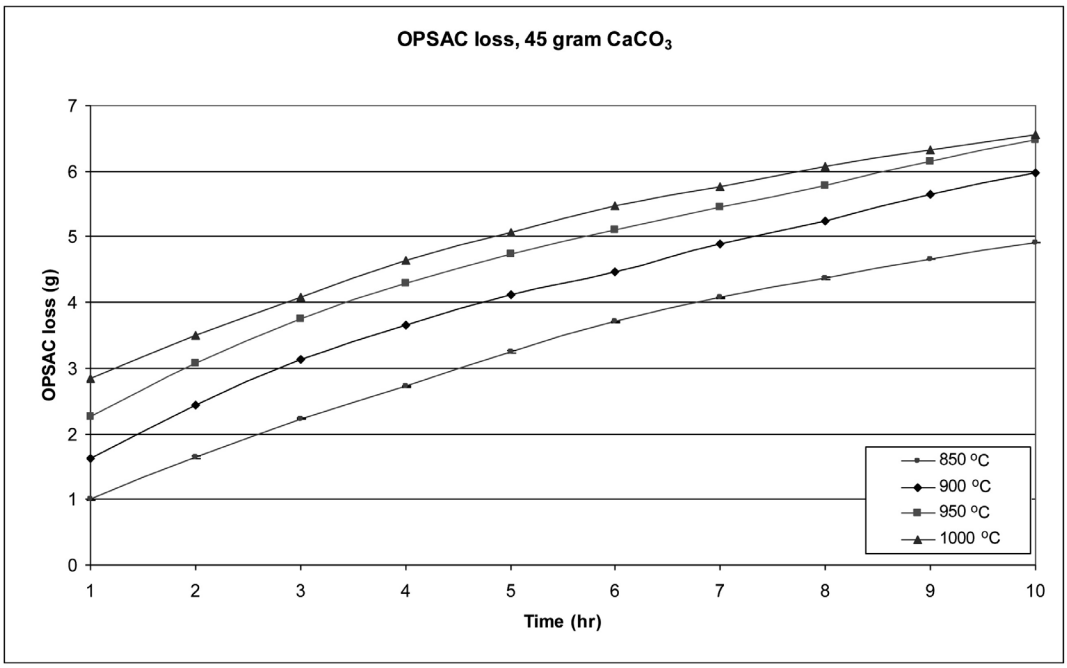

Figure 6: OPS Weight Loss, 45 gram $CaCO_3$.

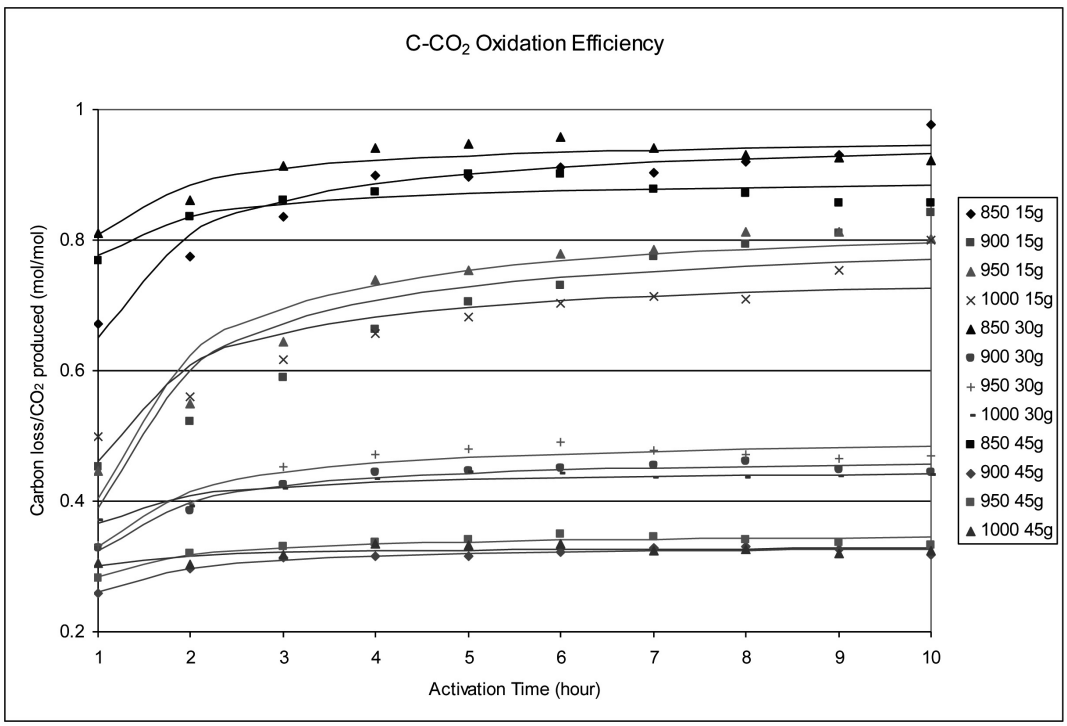

Figure 7: C-CO_2 Reaction Efficiency.

Table 2: OPS Weight Loss Statistical Results.

		15 g $CaCO_3$	30 g $CaCO_3$	45 g $CaCO_3$
850 °C	Turning Point Time (hour)	12.47	10.36	10.19
	Maximum OPS loss due to CO_2 (gram)	1.06	1.32	1.42
	C-CO_2 efficiency (%)	93.33	86.36	79.87
900 °C	Turning Point Time (hour)	9.5	7.95	7.77
	Maximum OPS loss due to CO_2 (gram)	1.25	1.55	1.68
	C-CO_2 efficiency (%)	82.36	47.79	33.64
950 °C	Turning Point Time (hour)	5.91	5.31	5.22
	Maximum OPS loss due to CO_2 (gram)	1.22	1.62	1.77
	C-CO_2 efficiency (%)	75.86	49.02	34.68
1000 °C	Turning Point Time (hour)	5.96	5.14	5.06
	Maximum OPS loss due to CO_2 (gram)	1.18	1.56	1.73
	C-CO_2 efficiency (%)	69.07	44.27	33.81

Table 2 shows the results of OPS weight loss due to CO_2 oxidation and their respective equilibrium points. For the same $CaCO_3$ weight, as the activation temperature increase, the activation time to reach maximum efficiency is reduced considerably, agreed to the trend of the CO_2 releases. When compared to different $CaCO_3$ weight, the weight loss was higher when $CaCO_3$ weight is higher. But, the oxidation efficiency decreases. This shows that not all of the released CO_2 is involved in the C-CO_2 reaction. Based on C-CO_2 reaction, one mol of CO_2 atom reacts with one mol C atom of the OPS. Thus, from the OPS loss gain, the quantity of the mol of CO_2 reacted to the carbon of the OPS is determined. The efficiency of the CO_2 is the quantity of the mol CO_2 reacted over the quantity of mol CO_2 released from the calcination process.

Figure 7 shows the OPS weight loss due to CO_2 gas oxidation over CO_2 released from calcination efficiency (mol/mol). At 850 °C, the efficiency is very high. This is due to the slow release of the CO_2, making it has enough time to react with the carbon atom. As the activation temperature increase, the CO_2 release is faster, making the reaction time with carbon atom shorter. Thus, the efficiency of CO_2 is gradually decreased. 15 g $CaCO_3$ sample had good efficiency of CO_2 regardless of the activation temperature, albeit lower OPS weight loss. However, the highest efficiency of the C-CO_2 reaction does not necessarily mean the highest OPS weight loss due to carbon oxidation. For example, the highest efficiency for activation at 850 °C is attained earlier than the highest OPS weight loss.

Adsorption Results

Figure 8 shows the result of adsorption capability of the generated OPSAC samples activated at 850 °C. The adsorption capability increase significantly at lower activation time and starting to equilibrate afterward. At lower activation time, additional to the release of the volatile matter due to heat, the C-CO_2 oxidation increased the weight loss, thus increasing the surface area. At higher activation temperature, the remaining volatile matter is diminished, making the activation is mostly factored by C-CO_2 reaction since the CO_2 gas continue to be released slowly even up to 10 hours calcination time. The results of adsorption performance for other activation temperature are shown in Figure 9. Each bar represented the highest adsorption value for each $CaCO_3$ weight. The adsorption capability increased significantly compared to

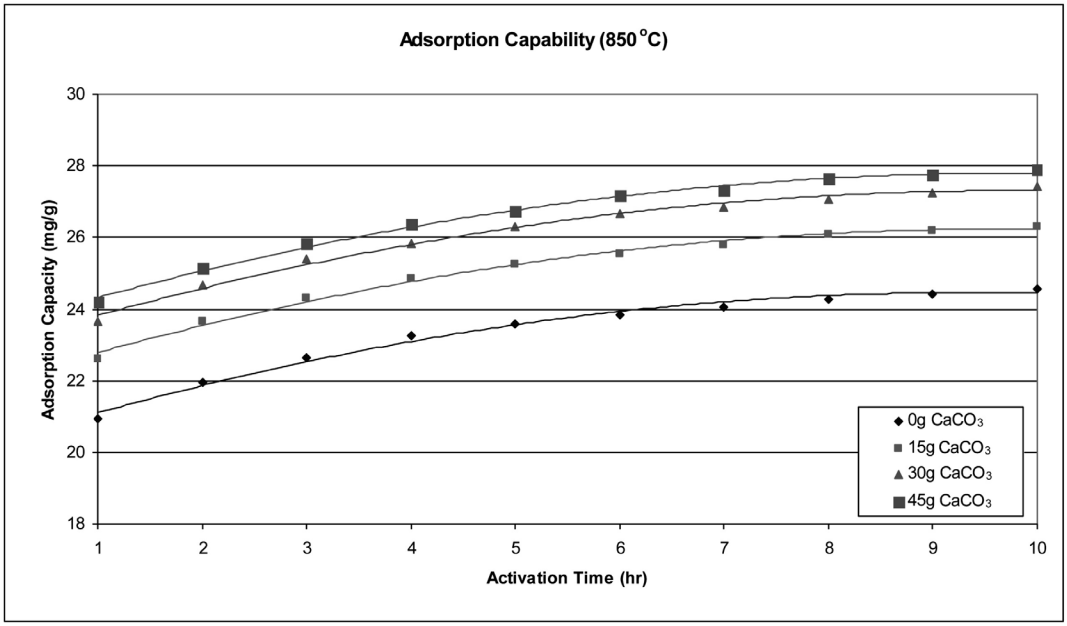

Figure 8: Adsorption Capability of the OPSAC, Activated at 850 °C.

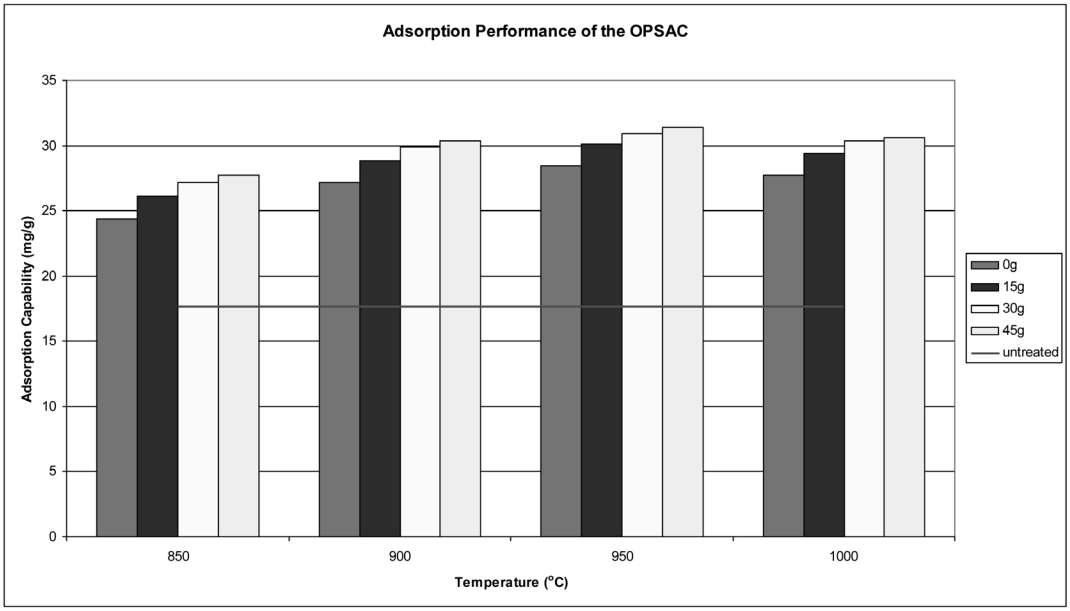

Figure 9: Max Adsorption Capability of the OPSAC.

Table 3: Statistical Result for Adsorption Capability of Generated OPSAC.

		0 g $CaCO_3$	15 g $CaCO_3$	30 g $CaCO_3$	45 g $CaCO_3$
850 °C	Turning Point Time (hour)	9.24	9.59	9.74	9.93
	Max Adsorption (mg/g)	24.38	26.14	27.17	27.72
	OPSAC loss (g)	3.32 22.1%	4.43 29.54%	4.74 31.6%	4.89 32.6%
900 °C	Turning Point Time (hour)	7.78	7.96	8.13	8.3
	Max Adsorption (mg/g)	27.2	28.86	29.85	30.35
	OPSAC Loss (g)	3.58 23.5%	4.88 31.9%	5.27 34.4%	5.42 35.8%
950 °C	Turning Point Time (hour)	7.2	7.4	7.5	7.6
	Max Adsorption (mg/g)	28.48	30.09	30.96	31.38
	OPSAC Loss (g)	3.77 25.1%	5.09 34.0%	5.48 36.5%	5.66 37.8%
1000 °C	Turning Point Time (hour)	6.13	6.19	6.23	6.19
	Max Adsorption (mg/g)	27.7	29.4	30.4	30.6
	OPSAC loss (g)	3.77 25.1%	4.97 33.1%	5.34 35.6%	5.49 36.6%

commercial OPSAC after being activated by the heat and the CO_2 gas. This proves that the commercial OPSAC is heated below 850 °C and without gas activation. The commercially available OPSAC only managed to adsorb 18 mg/g of CO_2, which corresponded to 47 m^2/g of S_{BET} covered surface area. It is slightly below of the adsorption at 0 °C which give a covered surface area of 59 m^2/g (Guo *et al*., 2001). Meanwhile, the generated OPSAC adsorption capability has been increased from 18 mg/g up to a maximum 31.38 mg/g. Activation on the heat alone, the capability is increased to 28.5 mg/g and the rest is by CO_2 gas activation. This proves that the generated OPSAC samples pore area has been significantly increased, making it more suitable for gas adsorption.

The adsorption capability of each sample against the activation time statistical results is represented in Table 3. From the estimated highest adsorption capability from 850 °C, 900 °C, 950 °C and 1000 °C activation, the maximum adsorption capability and the respective activation temperature was determined. The curve of adsorption capability against activation temperature shows a best fitting for the second degree polynomial equation. The equation is $y = -289.18 + 0.67x - 0.000353x^2$ with P-Value = 0.02 and R^2 = 99.97%. From this equation, the maximum adsorption capability is estimated at 31.4 mg/g when the OPSAC is activated at 953 °C. The polynomial relationship of $CaCO_3$ weight against activation temperature estimated the $CaCO_3$ needed is 46.87 gram to 15 gram OPSAC ratio. The linear equation of activation time against activation temperature estimated the activation time is 7.4 hour. However, the C-CO_2 oxidation efficiency at this point is the lowest, estimated at 34 %. High C-CO_2 reaction efficiency above 70% can be obtained when the activation is done at 850 °C or at 1:1 $CaCO_3$ weight ratio. But, the adsorption capability is reduced between 4 to 17% from the maximum adsorption value achieved.

Conclusion

The activation of the oil palm shell using the CO_2 emission from the $CaCO_3$ calcination is proved feasible. When the $CaCO_3$ is heated at minimum calcination temperature, the total CO_2 output is low. As the temperature increased, the efficiencies are also increased. The time to reach

these values also is getting shorter. The most effective C-CO_2 oxidation occurred at lower calcination temperature. The efficiencies are above 80%. However, the maximum adsorption capabilities are attained around 10 hour activation time. Higher carbon loss due to CO_2 oxidation could be attained if the activation temperature increased, but the C-CO_2 oxidation efficiencies will be reduced significantly, where most of the released CO_2 from the calcination is wasted as emission. A good efficiency above 70% also can be obtained at 1:1 weight ratio regardless activation temperature, but at extended activation time. At higher $CaCO_3$ weight ratio and higher activation temperature, the efficiencies are low. Anyhow the weight loss still continues beyond 10 hours activation time even the CO_2 released is depleted. After the CO_2 is fully released from $CaCO_3$ calcination, the activation continues on heat alone, releasing volatile matters instead of C-CO_2 oxidation.

The adsorption capability increased when the $CaCO_3$ weight is higher, regardless of the activation temperature. From the experiments, as the activation time increases, the adsorption capabilities demonstrate a second degree polynomial behaviour where a maximum point is attained. This shows that as the OPS weight decrease in the activation process, there is a point where the OPS weight loss is so severe that the total surface area per gram of the sample is reducing. As a result, the adsorption capability is reducing after certain activation time.

Conclusively, the synergetic process of the OPS activation and $CaCO_3$ calcination benefit two areas. CO_2 emission from the calcination process such as in the cement manufacturing can be captured by C-CO_2 reaction in the activation, while producing OPSAC at zero cost. From the point view of OPSAC manufacturing, the calcination serves as the activating agent. Calcium Oxide (CaO) by-product can re-use to sequestrate CO_2 emission and return back to carbonate form, making the process is fully recyclable.

Recommendations

This study focuses only on the heat and CO_2 gas activation of the OPSAC at a determined activation parameter and $CaCO_3$/OPS arrangement. The result of the carbon removal thus the adsorption capability could be different if the activation parameter and the $CaCO_3$/OPS arrangement during the calcination/activation process is different. The factors in the activation parameters such as granule size, the temperature of the OPS char preparation and even the type of the furnace and setting and the preparation of the OPS such as sieving method, cleaning method, soaking time and drying time is important. However, the most crucial is the arrangement of the $CaCO_3$ and OPS during the calcination/activation process. This will affect the performance of the calcination where the CO_2 is released and the exposed area of the OPS char during the activation. Higher rate of CO_2 production equally need a larger exposed OPS char surface area where the C-CO_2 oxidation can take place. As a result, the calcination/activation time could be faster and larger micropore area could be created.

References

Aik Chong Lua & Jia Guo. (2001). Preparation and Characterization of Activated Carbons from Oil-palm Stones for Gas-phase Adsorption. *Colloids and Surfaces A: Physicochemical and Engineering Aspects,* 179: 151-162.

Atanas Serbezov. (2001). Effect of the Process Parameters on the Length of the Mass Transfer Zone during Product Withdrawal in Pressure Swing Adsorption Cycles. *Chemical Engineering Science*, 56: 4673-4684.

B. R. Stanmore & P. Gilot. (2005). Review – Calcination and Carbonation of Limestone during Thermal Cycling for CO_2 Sequestration. *Fuel Processing Technology,* 86: 1707-1743.

Greenhouse Gas Inventory. Second National Communication to the UNFCCC, 2011. *p*.20.

Jia Guo & Aik Chong Lua. (2001). Characterization of Adsorbent Prepared from Oil-palm Shell by CO_2 Activation for Removal of Gas Pollutants. *Materials Letters*, 55: 334-339.

Jia Guo & Aik Chong Lua. (2002). Microporous Activated Carbons Prepared from Palm Shell by Thermal Activation and Their Application to Sulfur Dioxide Adsorption. *Journal of Colloid and Interface Science*. 251**:** 242–247.

Malaysia Palm Oil Board. (2007). Planted Area and Yield, Malaysia Palm Oil Statistics. Retrieved from http://econ.mpob.gov.my/ economy/ annual/ stat2007/ EID_ statistics07.htm.

M. Harimi, M. M. H Megat Ahmad, S. M. Sapuan & Azni Idris. (2004). Numerical Analysis of Emission Component from Incineration of Oil Palm Wastes. *Biomass and Bioenergy,* 28: 339-345.